USING PILOTED SIMULATION TO MEASURE PILOT WORKLOAD OF LANDING A HELICOPTER ON A SMALL SHIP

Paul Scott, Michael F Kelly, Mark D White, Ieuan Owen

School of Engineering
University of Liverpool
Liverpool, UK

Abstract

When conducting landings to a ship's deck in strong winds, helicopter pilot workload is often dominated by the turbulence within the ship's airwake. Previous studies have shown that larger ships create more aggressive airwakes and simulated flight trials had shown that it can be easier to land to a smaller ship than a large one. However, there are helicopter-enabled ships that are less than 100m in length and these will have significantly greater ship motion in rough seas than a large ship. The study reported in this paper has used a motion-base flight simulator to evaluate the pilot workload when landing to three geometrically similar ships of lengths 100m, 150m and 200m. Ship motion software has been used to create realistic deck displacements for sea states 4, 5 and 6, which are consistent with the increasing wind speed over the deck. It has been shown that the 100m ship was the most difficult to land to, with deck motion being the limiting factor. The next most difficult ship to land to was the 200m ship, with airwake turbulence being the limiting factor. The 150m ship generated the lowest pilot workload. The study has demonstrated that when ship motion is excessive, as it will be with small ships in rough seas, pilot workload will be dominated by deck motion during a landing task, but as the ship gets larger and more stable, airwake disturbances will dominate. It is clear from this study that realistic ship motion is essential when using piloted flight simulation to conduct simulated ship-helicopter operations.

1. INTRODUCTION

It is now commonplace for helicopters to operate to naval ships such as frigates and destroyers and there are increasing applications of helicopters operating to smaller patrol vessels. While a destroyer may have a typical length of 150m, the length of a helicopter-enabled patrol vessel may only be half of that. For example, HMS Clyde, a UK River-class patrol vessel is 82m long, and its helicopter deck, which is just 24m in length and 13m wide is designed to accommodate a 23m long AW 101 Merlin helicopter. A graphic of HMS Clyde with a Merlin Helicopter on the flight deck is shown in Fig. 1 [1].

Figure 1 Graphic of HMS Clyde, a River-class Patrol vessel with a Merlin helicopter on the flight deck

The next generation UK frigate will be the City class Type 26, an early design version of which is illustrated in Fig. 2 [2]. The helicopter shown in Fig. 2 is again a Merlin so the relative proportions of the landing deck to the helicopter can be seen. It is expected that the ship will be 150m in length and its landing deck will be about 31m long and 20m wide, so providing the pilot a significantly larger deck than in Fig.1.

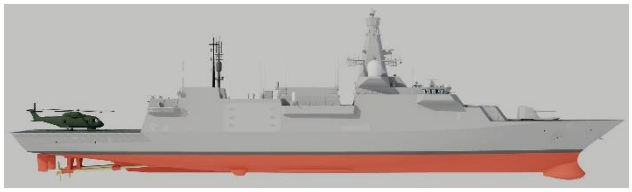

Figure 2 Future UK City class Type 26 frigate with a Merlin helicopter on the flight deck

The difficulty of flying a helicopter to the moving deck of a ship in adverse weather conditions is well documented, e.g. [3]. The main challenges to the pilot come from the small landing area that has considerable movement in heave, pitch and roll in rough seas; from the highly unsteady turbulent air flow over and around the flight deck; and from the close proximity of the ship's superstructure. While

there are other adverse effects, such as poor visibility and hot exhaust gases from the ship's engines, the three main effects are those listed above with pilots usually commenting that turbulent air flow is the primary limiting factor for a safe landing in rough weather. The turbulent air flow over the ship is known as the ship airwake, and its characteristics are governed by the ship topside geometry, and the speed and the angle of the wind relative to the ship. The aerodynamics of ship airwakes have been extensively studied through both wind tunnel testing and Computational Fluid Dynamics (CFD), e.g. [4,5].

The demanding nature of ship-helicopter operations means that each ship and helicopter combination is subject to its own specific Ship-Helicopter Operating Limits (SHOL) which specifies the limiting wind strength and direction for which it is safe to launch the helicopter [6]. SHOLs are normally determined during the ship's First of Class Flight Trials (FOCFT) which are inherently costly and dangerous to carry out, requiring aircraft to be flown to the limits of what is considered safe, and often beyond the capabilities of the average fleet pilot. Due to these shortcomings associated with the FOCFTs, considerable research has been conducted, at the University of Liverpool (UoL) and elsewhere, into using flight simulation to support, or possibly replace, SHOL testing [7,8,9].

The Flight Science and Technology Research Group at the UoL has developed rotorcraft flight simulation research facilities with the over-arching aim of improving the fidelity of flight simulation, with particular attention being paid to the helicopter-ship dynamic interface. Much of this work has involved the use of the HELIFLIGHT-R motion-base flight simulator, shown in Fig. 3 [10]. The simulator features a three-channel 220° x 70° field of view visual system, a six degree of freedom motion platform, a four axis control loading system and has an interchangeable crew station. As well as the usual simulation environment, i.e. visual and aural cues, full motion, and aircraft flight mechanics models, an unsteady CFD-generated airwake is also provided to disturb the aircraft when it is within the ship's airwake [8,9].

Using piloted flight simulation, Forrest et al. [8] compared the simulated SHOLs of the UK's Type 23 naval frigate and the larger Wave class tanker. It was found that although the tanker has a much larger deck area, it had a more restricted SHOL than the Type 23 frigate due to the larger turbulent flow structures shed by the larger superstructure. The increased energy contained within the turbulent flow over the tanker in turn increased the level of pilot workload. Although the two ships were substantially different in shape, the conclusion was that larger ships created more problematic airwakes. Considering the relative difficulty of landing a helicopter to the 24m x 13m deck of the patrol vessel in Fig. 1 compared with the 31m x 20m deck of the frigate in Fig. 2 it is not therefore necessarily the case that the smaller landing deck will pose the greatest challenge to the pilot.

Figure 3 The University of Liverpool HELIFLIGHT-R motion base research simulator

To explore further the effect of ship size on the airwake and on the helicopter, Scott et al. [11] used CFD-generated airwakes coupled with a helicopter flight model to show that, as the ship gets smaller, the airwake becomes less aggressive for the helicopter compared with the airwake from a larger ship. This is because the ship superstructure is an assembly of bluff bodies (e.g. mast, funnel, bridge, hangar) that shed unsteady wakes. As the bluff bodies get smaller the size of the shed vortices become proportionally smaller and their frequency of shedding becomes proportionally higher. The net result is that the smaller, higher frequency aerodynamic disturbances contribute less to pilot workload [12]. However, while the study showed that the airwake is less challenging for the helicopter pilot as the ship gets smaller, the landing deck also becomes smaller and the proximity of the superstructure becomes more threatening. It was still not immediately obvious from this study therefore, whether smaller ships are easier for a pilot to land a helicopter to, or harder.

To examine further the effect of ship size on the difficulty of landing to the ship, Scott et al. [13] went on to conduct simulated flight trials in the HELIFLIGHT-R motion simulator in which a pilot carried our deck landings to the three geometrically similar ships shown in Fig. 4. The ships have a generic geometry that is typical of modern warships

and the lengths of the three ships are 100m, 150m and 200m. The helicopter model used in the flight tests was representative of a SH-60B Seahawk. Figure 5 shows the size of the helicopter rotor relative to the 100m and 200m ships; also shown in this figure is the turbulence intensity in the ships' airwakes for a head wind. It can be seen that the helicopter rotor is exposed to more turbulent flow over the larger ship.

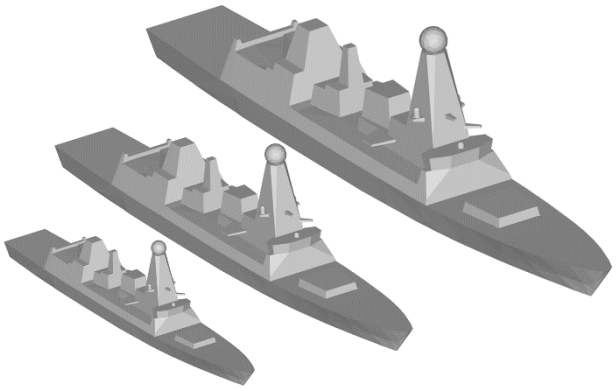

Figure 4 The generic naval frigate geometry and the range of ship sizes used for this study (lengths 100m, 150m, 200m).

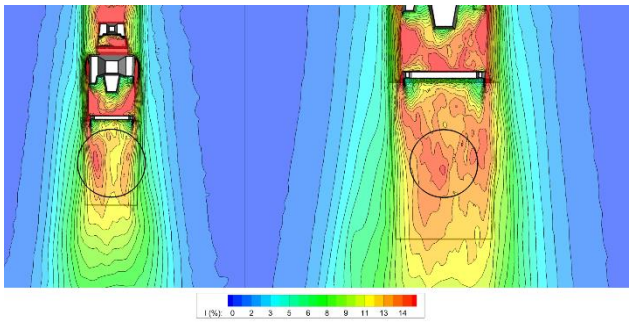

Figure 5 Relative size of 100m and 200m ship flight decks showing SH60-B rotor diameter and CFD-generated turbulence intensity at hangar heights.

In the flight tests reported in [13] the three ships had the same deck motion and while it was recognised that different size ships will have different dynamic responses to a given sea state, it was decided to use the same deck motion for each ship size so that the flight tests were able to distinguish the pilot workload required to land to a small and large ship due only to their airwakes and to the size of their landing decks. The results from the flight trials showed that pilot workload generally increases with ship size and that, despite the landing area being larger and the superstructure proximity being less threatening, the more aggressive airwake still makes the aircraft more difficult to control over the larger ship. During the flight trials, however, the pilot commented that the same ship motion for the different size ships while in the same sea state was unrealistic. Therefore, a new set of flight trials was planned in which the sea state was different for different wind strengths, and the ship motion for each ship size shown in Fig. 4 was used in the simulations. The purpose of this paper is to report a selection of the results of the simulated flight trials for the three ships shown in Fig. 4 in a headwind with different wind strengths and ship motions.

2. CREATING SHIP AIRWAKES IN CFD

To produce the flight simulation environment a generic ship model was created to represent a modern, single-spot naval frigate with a beam of 20m and a length of 150m. This geometry was then scaled to produce two ship models of 100m and 200m in length, creating the ships shown in Fig. 4 and which span the size range of single-spot combat ships that operate with maritime helicopters.

The unsteady airwake was created using ANSYS Fluent, a commercial CFD code. The ship model was imported into the ANSYS ICEM mesh generation software, so that it could be 'cleaned' to repair any erroneous surfaces and to remove small features to create geometry suitable for meshing. Features such as small antennae, railings and other small deck clutter have little effect on the airwake but if not removed will increase the complexity and hence the run-time of the CFD. Generally, objects that are less than 0.3m in diameter were removed. A surface mesh was then applied to the ship geometry and this was 'grown' away from the ship into the computational domain which surrounds the ship. Figure 6 shows a cross-sectional view of the mesh close to the ship.

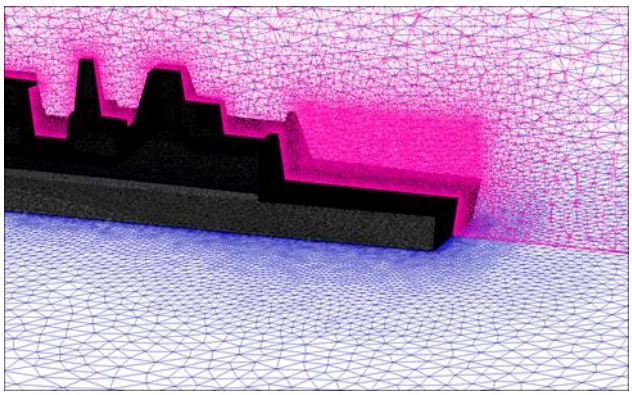

Figure 6 Computational mesh used to produce the CFD simulations, note the refinement region over the flight deck

Areas of particular interest within the volume mesh, such as the flow aft of the hangar and the area

adjacent to the flight deck, were further refined using regions of high density mesh to increase the resolution of turbulence within the airwake, the total cell counts were in the region of 15 million cells. The unsteady CFD airwake was computed using Detached Eddy Simulation (DES) turbulence modelling. Thirty seconds of unsteady airwake were computed at 100 Hz for the 150m ship at a 40 knots wind speed for different wind angles. Further details of the CFD methodology and experimental validation has been described by Forrest and Owen [5].

Having created the three-dimensional unsteady velocity components at every 0.01 seconds, the velocity components can then be scaled for different ship sizes and wind speeds, so saving substantial computing time and resources. Scott et al. demonstrated the validity of the scaling process in [13]; for the present study ship size was scaled from the 150m ship to the 100m and 200m ships, and the wind speed from 40 knots to velocities between 15 knots and 60 knots. The vortices shed from bluff bodies within a flow are created at distinct frequencies which can be described by the Strouhal Number (Reynolds number dependence is acknowledged, but is known to be less important at high values and for sharp-edged bodies). Strouhal number relates the characteristic length of a bluff body, l, the flow speed v, and the frequency, f, of the vortices shed from the body ($St = f\ l/v$) This simple relationship shows that for an increase in free stream flow speed there will be a proportional increase in shedding frequency, and for an increase in length scale there will be a proportional decrease in frequency. While this may be obvious for vortex shedding at a single frequency, the principle can also be extended to more complex shedding from the multiple bluff bodies that make up a ship's superstructure. Therefore, the airwake velocity components for the different wind speeds and ship sizes were scaled from the 40 knot airwake for the 150m ship. Note that separate airwakes were computed for different wind angles. The airwake was 'connected' to the ship geometry so that it moves with the ship.

3. SHIP MOTION

The motions of the three ships at sea were simulated using ShipMo3D, a well-validated ship motion potential-flow code developed at Defence Research and Development Canada (DRDC) – Atlantic, and made available to the UoL. ShipMo3D predicts ship motion based on the Green function for zero forward speed, and was selected due to its well-documented validation for vessels travelling at moderate speed (i.e. Froude numbers below 0.4), via both model testing and full-scale at-sea trials [14]. Further, ShipMo3D has been designed to facilitate interoperability with other software, lending itself well to use in a distributed simulation environment such as is used in this study [15]. Validation has shown ShipMo3D can predict RMS motions to typically be within 10 to 30 percent of observed values, with heave predictions being the most accurate and roll predictions being the least accurate.

3.1. Ship Geometry

Geometry representative of the hull of the 150 m long ship was input into ShipMo3D as a set of hull surface coordinates. Ship appendages were also included, with the hull featuring a bulbous bow, two rudders, two propellers, two bilge keels, two roll stabilisers, and a skeg. The hulls and their appendages were linearly scaled in size to match the 100 m and 200 m ships, and while it is acknowledged that hull appendages will not necessarily be linearly scaled with ship length, appendages were scaled in this manner to maintain a better comparison between the three ships. The draught, height of centre of gravity above baseline (KG), and thus metacentric height (GM) were also scaled; these values are given for each ship in Table 1. Roll gyradius was assumed to be 35% beam, while pitch and yaw gyradii were taken as 25% ship length.

Table 1 Scaled ship properties

Length (m)	**100**	**150**	**200**
Beam (m)	11.7	17.6	23.4
Displacement (t)	2,380	8,040	19,057
Draught (m)	4.0	6.0	8.0
GM (m)	1.2	1.8	2.4
No. Panels (wetted hull)	1192	1342	1382
Prop. Dia. (m)	2.67	4.0	5.33
Prop. RPM (@ 12kts)	162.3	106.5	79.2

Once input into ShipMo3D, the hull surface coordinates were panelled as a solid surface using triangular and quadrilateral panels, with a minimum 1000 panels representing the wetted hull to ensure grid independence; the number of panels used on each of the three ships is given in Table 1. The panelled geometries are shown in Fig. 7. The wet and dry hull panels are shown as yellow and green, respectively, with the hydrostatic waterline located at the interface between these surfaces.

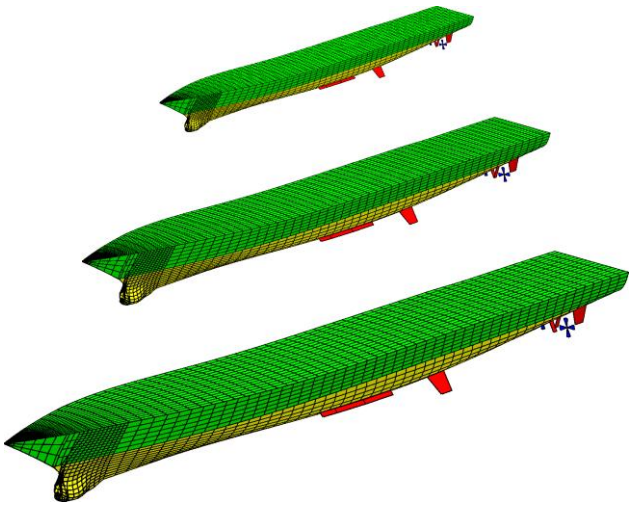

Figure 7 Panelled hulls, with appendages

3.2. Seaway Generation

For the piloted flight trials, three random seaways were generated representing sea states 4, 5, and 6, using the Bretschneider spectrum [16], which is widely used to model point wave spectra in the open ocean. Significant wave heights ($H_{⅓}$) and peak wave periods (T_p) used for each sea state are given in Table 2. For a 12 knot ahead ship speed, sea states 4, 5, and 6 were taken as representative of conditions encountered in the North Atlantic for the Wind Over Deck headwinds tested in this study.

Table 2 Conditions for sea states 4-6

WOD (kts)	Sea State	T_p (s)	$H_{⅓}$ (m)
15, 25	4	8.8	1.9
35, 40	5	9.7	3.3
45, 50	6	12.4	5.0

While a unidirectional Bretschneider spectrum can be used to approximate long-crested oceanic waves, lateral motion (roll, sway, and yaw) will be absent due to the symmetry of the ship geometry travelling directly into two-dimensional waves, and so a cosine-squared spreading function was implemented with a 90° spreading angle and 15° heading interval, as supported by trials evidence for typically occurring conditions in the open ocean [17]. In this way a more representative short-crested wave spectrum was generated, represented by eleven reduced Bretschneider spectra distributed around the dominant ahead wave direction; this has the advantage of imposing realistic lateral forces upon the symmetrical ships in the ahead case that cause the ships to roll, which they would not do in a unidirectional wave spectrum.

3.3. Ship Motion Computations

Once the ship geometries had been successfully panelled and all load condition data specified, the three differently sized ships were placed into the same three simulated head waves at 12 knots ship speed for a total time period of 180 seconds, with the first 60 seconds discarded as a settling period to allow ramping up of ship motions from rest.

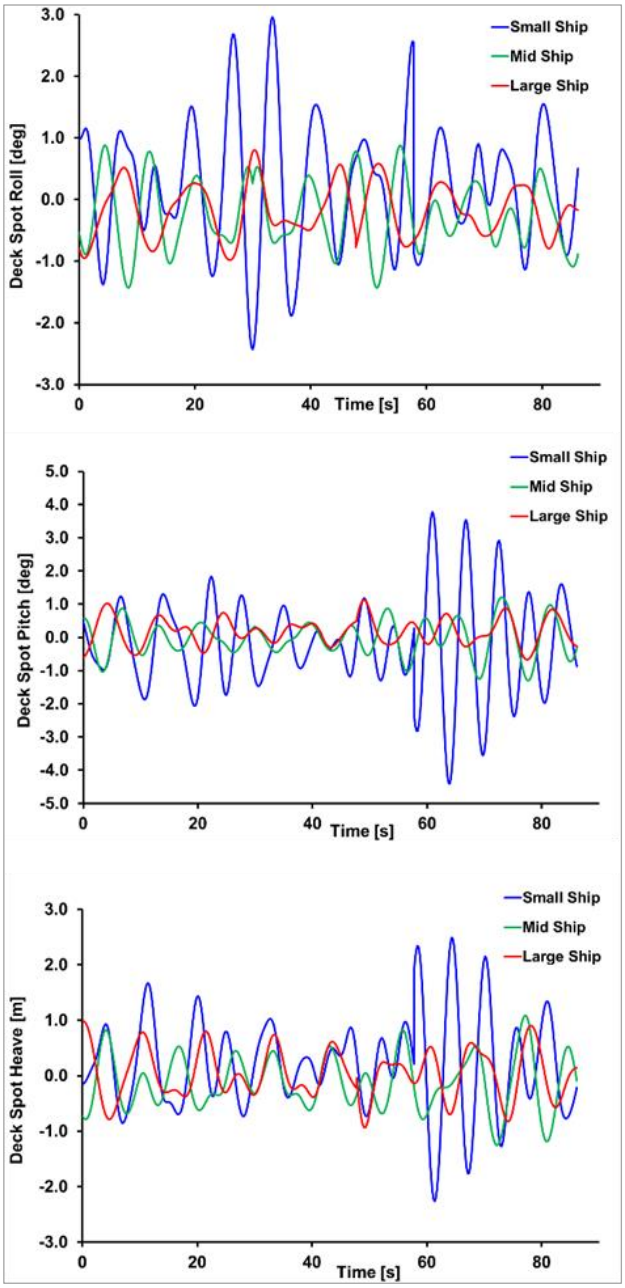

Figure 8 Computed displacements of the landing spot for the three ships travelling at 12 knots through sea state 5 with waves coming from ahead

The ship motion was calculated as roll, pitch and heave at the ship's centre of gravity. These were then imported into UoL's flight modelling and simulation environment, FLIGHTLAB, which creates a deck contact area for launch and recovery operations. The ship motion data is broadcast across a local network to drive a visual model of the ship in UoL's run-time environment, LIVE. Landing spot state information i.e. attitudes, velocities and accelerations, are recorded in FLIGHTLAB during piloted simulation trials. Figure 8 shows an example of the deck motion (roll, pitch and heave) at the landing spot for the three ships travelling at 12 knots through sea state 5, with the waves coming from ahead. Looking at the small ship data, maximum roll and pitch are about ±3˚, and maximum heave is about ±2m, compared with less than ±1˚ pitch and roll, and about ±1m for the large ship. It can also be seen in Fig. 8 that there are periods in the ship motion that are less violent than others and it is these naturally occurring quiescent periods that the pilot waits for when executing a landing.

4. PILOTED FLIGHT SIMULATION

The creation of a full-motion flight simulation environment for a helicopter operating to a ship requires: a simulator, in this case the HELIFLIGHT-R shown in Fig. 3; a ship visual model, such as in Fig. 4, suitably rendered; a CFD-generated airwake; a ship motion model; a visual scene; and a helicopter flight dynamics model.

The helicopter flight dynamics model was provided by Advanced Rotorcraft Technology's (ART's) FLIGHTLAB software [18]. Motion base acceleration commands to the HELIFLIGHT-R simulator are provided as outputs from the aircraft flight dynamics model through a motion drive algorithm. A fully programmable control loading system provides force-feedback through the aircraft cyclic, collective, and pedal inceptors. CFD airwakes can be integrated with FLIGHTLAB, enabling unsteady airwake velocities to be imposed upon the aircraft flight model. During testing, FLIGHTLAB allows real-time data monitoring and recording which, together with in-cockpit video and audio recordings, are used for post-trial analysis.

The FLIGHTLAB Generic Rotorcraft model used for this research was configured to be representative of the Sikorsky SH-60B Seahawk, a maritime development of the widely used UH60 Black Hawk. The model is constructed from a set of modular components such as the rotor, fuselage and turbo-shaft engine. The unsteady airwake data is integrated into the helicopter flight dynamics model by applying the time varying velocity components to the aircraft via a number of Airload Computation Points (ACPs) which are located at various points along each rotor blade, fuselage, tail rotor and empennage, as shown in Fig. 9.

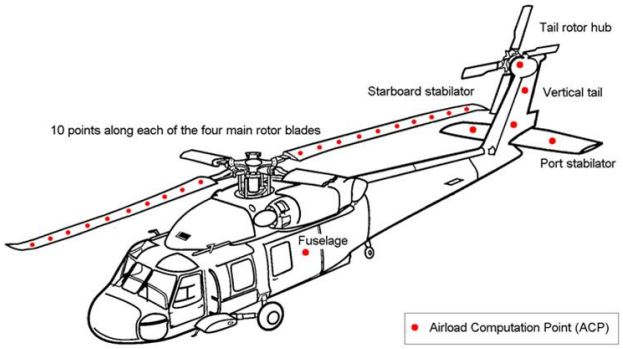

Figure 9 Location of the ACP's used on the SH60-B helicopter flight dynamics model in FLIGHTLAB

Each CFD simulation produces thirty seconds of unsteady CFD data, generated on a high density, unstructured mesh. Due to memory constraints when running real-time piloted simulations, the computed airwake data requires post-processing before it can be used within FLIGHTLAB. Reduction of the airwake data size is undertaken by first sampling the 100Hz data at every fourth time step and then by interpolating the unstructured CFD data onto a structured mesh using a grid spacing of 1 metre, covering a region of interest around the flight deck of the ship. The 30 second airwake data was looped smoothly for the duration of the flight test.

FLIGHTLAB includes a dynamic inflow model and also accounts for the downwash from the rotor. However, the interaction between the airwake and the rotor model is not fully coupled, i.e. it is 'one-way', such that the helicopter is affected by the airwake, but the rotor downwash does not interact with the airwake.

A comprehensive description of the simulated SHOL testing process can be found in [9].

4.1. Test Procedure

The flight tests were conducted by a former UK Royal Navy helicopter test pilot. The landing tasks were based on the Royal Navy port-side approach where the pilot brings the helicopter to a forward-facing hover position alongside the landing deck, approximately one beam width off the port side of the ship, matching the speed of the ship. The pilot then conducts a lateral translation to a hover over the deck landing spot before descending to land on the flight

deck. During the tests, the pilot was asked to hold a hover position over the port edge of the flight deck at approximately hangar height for thirty seconds and to provide a rating of the workload experienced; this was followed by a thirty second hover over the flight deck, again with an evaluation of the workload. During the testing, the pilot was given the flexibility to adjust altitude as deemed fit to accommodate the ships' deck motions.

The pilot was asked to provide workload ratings for the individual hover tasks using the Bedford workload ratings scale [19]. The Bedford workload rating scale is a 10-point scale used by evaluation pilots to assess the workload required (by an 'average' pilot) to successfully complete a given task. Ratings 1-3 are awarded when the workload is considered to be satisfactory without reduction and does not prevent the pilot from performing additional tasks (e.g. monitoring aircraft systems or radio communications). Ratings of 4-6 are awarded where workload is deemed to be tolerable for the task, while a rating of 7-9 is awarded where the task can be performed successfully, yet the workload is not tolerable for the task. Finally, a rating of 10 is awarded in situations where the pilot is unable to complete the task, and so must abandon it.

The pilot was also required to provide a rating from the Deck Interface Pilot Effort Scale (DIPES) [20] for the overall difficulty of the complete landing task. The DIPES scale requires the test pilot to give a rating of 1-5 for any given launch/recovery task. A rating of 1-3 is considered to be acceptable, with the task considered to be within the abilities of an average fleet pilot. Conversely, a rating of 4 is deemed to be unacceptable on the basis that an average fleet pilot would not be able to complete the task in a consistently safe manner, while a rating of 5 indicates that the task cannot be safely completed by the test pilot even under controlled test conditions. Additionally, the test pilot can apply one or more letter suffixes to a DIPES rating which describe the cause(s) of the increased workload e.g. T for turbulence.

More complete descriptions of the Bedford and DIPES workload rating scale and their use in flight simulation can be found in [9].

Flight tests were conducted for each ship size and for a number of wind conditions. The results presented in this paper are for the headwind condition with wind speeds from 15 to 50 knots.

4.2. Results

The Bedford workload ratings for each of the three ships for the headwind case are given in Fig. 10, for the thirty second, deck spot hover task. As the wind speed over the sea increases, so the sea state can be expected to increase. In this case the expected sea state for the wind speed is shown on the graph, and the motion of each ship was computed, as described in Section 3, for that sea state and a ship forward speed of 12 knots.

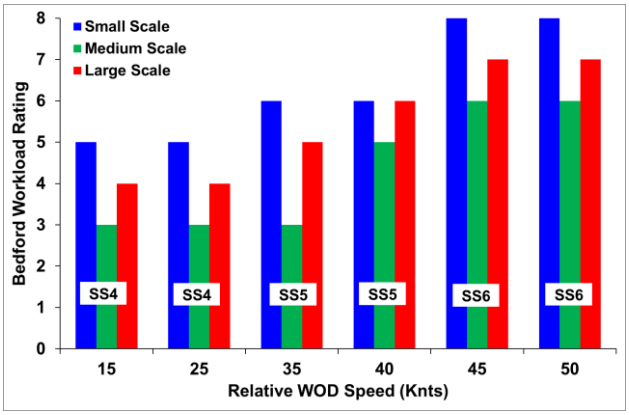

Figure 10 Bedford workload ratings awarded in current tests by pilot for the hover task above the deck spot, headwind, realistic ship motion, 12 knots ship speed.

It can be seen in Fig. 10 that, for all three ships, the workload required to maintain the hover over the moving deck increased as the wind strength increased. This is because the helicopter is immersed within the turbulent airwake and the unsteady loads being imposed on the aircraft will increase as wind speed increases. Also, as the wind speed increases so too does the sea state and the displacement of the ships' deck. It can also be seen that the workload required to hold the hover position over the small ship is higher than for the medium and large ship. This is despite the fact that the small ship's airwake is the least aggressive, and the higher workload must therefore be due to the large displacements of the small ship's deck with some additional workload arising from the airwake disturbances. It can also be seen in Fig. 10 that the large ship has generated workload ratings that are generally one rating less than those awarded for the hover task over the small ship and one rating higher than those awarded for the medium size ship. In each case the minimum workload rating is awarded for the medium size ship. The pilot is having to contend with both the deck motion and the airwake and it appears that the 150m ship (which is typical of a single-spot frigate) has the best combination of moderate deck motion and airwake. The small ship has the least aggressive airwake, but the greatest deck motion, and the large ship has the most aggressive airwake and least deck motion.

These results can be compared with similar tests reported in [13] where the same ships and airwakes were used, but the ship motion was the same for all three ships so that the airwake effect could be seen in isolation. In [13] the ship motion was representative of the medium ship in a sea state 3. The results of the workload ratings awarded for the hover task can be seen in Fig. 11 below; again workload can be seen to increase with wind speed, but with much lower values than in Fig. 10, and in the case where the pilot does award higher ratings for a given wind speed it is for the smaller ship, where the pilot reported the close proximity of the hangar as an issue. It is clear from comparing Figs. 10 and 11 that realistic ship motion is essential for simulated landings of a helicopter to a ship.

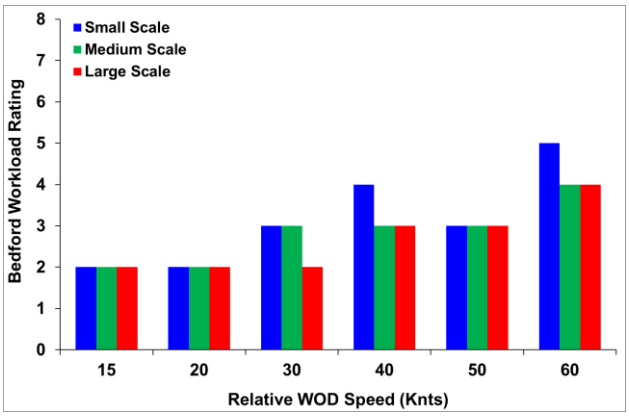

Figure 11 Bedford workload ratings awarded in previous tests [13] by pilot for the hover task above the deck spot, headwind, with equal and limited ship motion.

Further insight into the difficulty of holding the helicopter in a stable hover over the landing spot can be gained by looking at the control activity of the pilot during the hover task. Figure 12 shows the pilot's cyclic control inputs, which are used for lateral and longitudinal positional control during the 30 second hover over the landing spot. The largest excursions are for the large ship and will be due to the larger, slower moving vortices being shed from the ship superstructure. The smaller ship shows the smallest excursions while the control activity for the medium ship lies between the two.

The data in Fig. 12 does not explain why the pilot awarded the greatest workload ratings to the hover task over the smallest ship. However, Fig.13 shows the pilot's control inputs to the collective, which provides power and thrust to main rotor (and which then also interacts with the pedal control as the aircraft changes attitude in yaw). It can be seen in Fig. 13 that the greatest activity in the collective control is for the hover task over the small ship, while the lowest is for the large ship. As the small ship's airwake is the least disruptive the pilot is therefore having to work hard to hold vertical position over the landing spot as the ship moves about violently, as seen earlier in Fig. 8. The same situation is seen in the pedal control activity in Fig. 14 where the largest excursions are seen over the small ship.

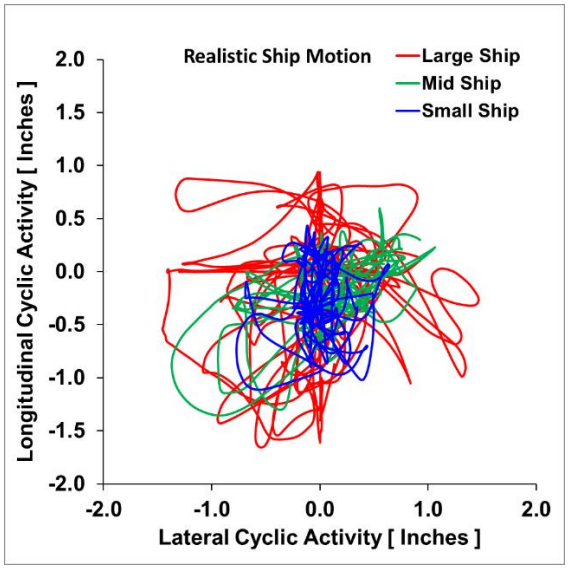

Figure 12 Cyclic control activity during hover task over landing spot for a 40 knot headwind, sea state 5.

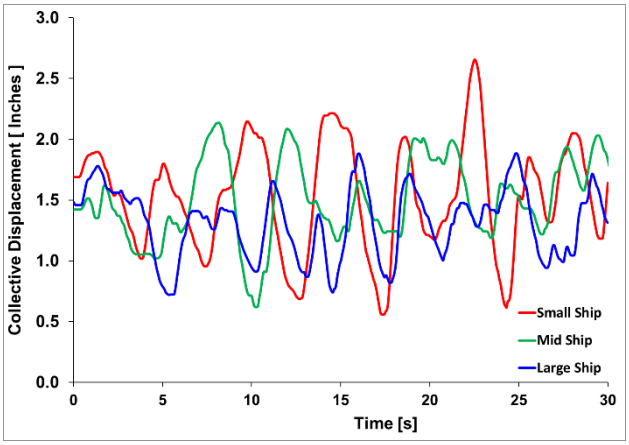

Figure 13 Collective control activity during hover task over landing spot for a 40 knot headwind, sea state 5.

Bearing in mind that while holding position over the landing spot the pilot is also being exposed to visual cues with the smaller ship moving in significant roll, pitch and heave, especially when compared with the slower motion of the larger ship. The combination of control activity and cueing information the pilot is contending with means that, as Fig. 10 shows, the workload is highest for the smaller ship and is lowest for the medium ship.

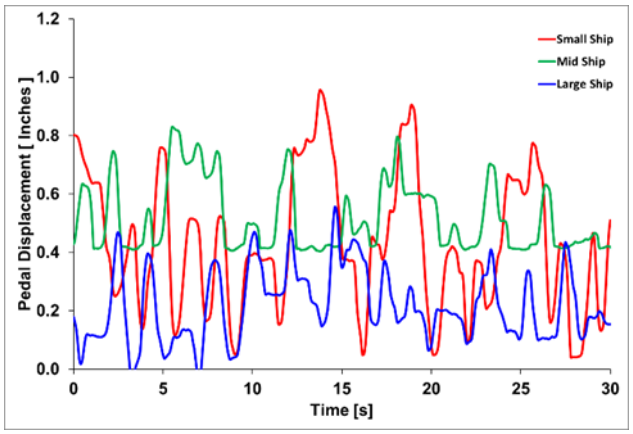

Figure 14 Pedal control activity during hover task over landing spot for a 40 knot headwind, sea state 5.

Finally, the pilot was also asked to rate the difficulty of the whole landing task using the DIPES scale. In this task the pilot began with the helicopter alongside the ship, off the port side; the helicopter was then translated across the deck and held in the hover position over the spot until the pilot deemed it appropriate to land. The DIPES ratings awarded by the pilot for headwind speeds from 15 to 50 knots and for the three ship sizes with appropriate sea-state motion are shown in Fig. 15. Again, it can be seen that in general the pilot's workload increase as the wind speed increases, and the greatest effort is required for the landing to the smaller ship. It should also be noted that the safe limit for the landing task is 3 so that for a headwind of 45 knots it is unsafe to land to the small ship, and for a headwind of 50 knots it is unsafe to land to the small and medium ships.

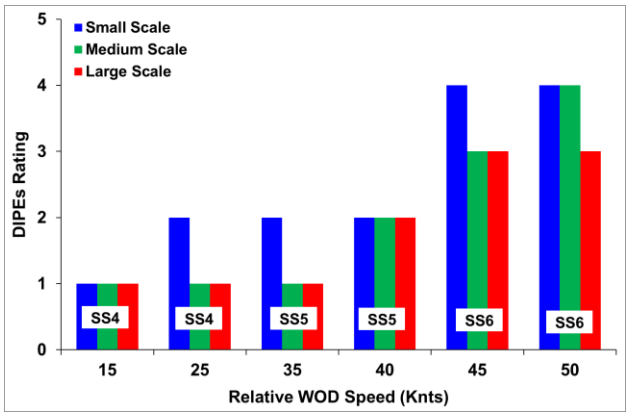

Figure 15 DIPES ratings awarded in current tests by pilot for the landing task. Headwind, with realistic ship motion.

As well as awarding the DIPES ratings in Fig. 15, at higher workload the pilot also identified the causes. For the large ship the pilot indicated that fore-aft positioning and turbulence were the limiting factors. For the smaller ship the limiting factors were difficulty of ship tracking and positional accuracy as well as torque limit while trying to track the deck vertically; i.e. ship motion was the determining factor. For the medium ship the pilot reported that a combination of turbulence and ship motion made it difficult to hold position.

Figure 16, extracted from the earlier study reported in [13], shows the DIPES ratings awarded to the landing task when the ship motion was the same for all three ships, i.e. a relatively low motion corresponding to that of the medium ship in a sea-state 3. As reported in [13], the pilot awarded the lowest DIPES rating of 1 for all three ships up to a headwind speed of 40 knots, and at wind speeds above this the greatest effort was awarded for the deck landings to the larger ships confirming that when ship motion is not an issue it is the unsteady aerodynamic loads on the aircraft due to the airwake that dominates the pilot's workload.

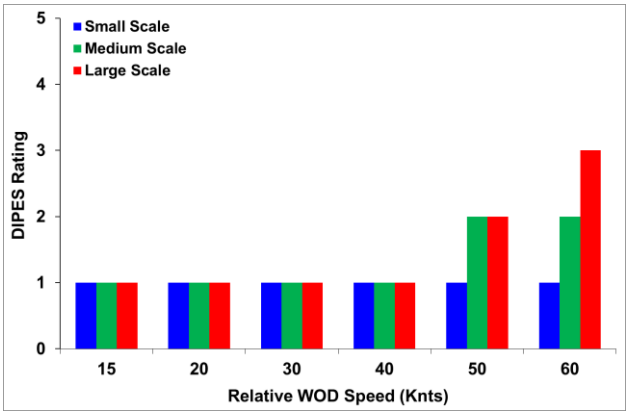

Figure 16 DIPES ratings awarded in previous tests [13] by pilot for the landing task. Headwind, with equal and limited ship motion.

5. CONCLUSIONS

Previous studies have shown that larger ships create more aggressive airwakes and simulated flight trials had shown that it can be more difficult to land to a large ship than a smaller one, even though it had a bigger landing deck; i.e. the landing task was dominated by the ship airwake. In those tests, however, the deck motions of the large and small ships were the same. In the study reported in this paper, realistic ship motion for three different size ships has been computed for sea states that are consistent with the relative wind over the ship.

Three geometrically similar ships of length 100m, 150m and 200m have been considered. With the realistic ship motion included, flight simulation

showed that workload was highest when landing to the smaller ship and lowest when landing to the medium size ship. It cannot be said therefore that as the ship gets larger the landing gets more difficult, but when ship motion is significant the moving deck provides a greater challenge to the pilot than does the airwake. With larger ships, the deck motion presents less of a challenge, while the unsteady loads from the airwake dominate the pilot's workload.

It is clear from this study that realistic ship motion is essential when using piloted flight simulation to conduct simulated ship-helicopter operations.

References

1. Royal Navy website, accessed July 2017, http://www.royalnavy.mod.uk/our-organisation/the-fighting-arms/surface-fleet/patrol/river-class/hms-clyde
2. Royal Navy website, accessed July 2017, http://www.royalnavy.mod.uk/the-equipment/ships/future-ships/type-26
3. Lumsden, B. and Padfield, G.D. "Challenges at the Helicopter-Ship Dynamic Interface", Military Aerospace Technologies – Fitec ' 98, IMechE Conference Transactions, Institute of Mechanical Engineers, Wiley, UK, 1998.
4. Polsky, S.A. and Bruner, C.W.S. "Time-Accurate Computational Simulation of an LHA Ship Airwake", AIAA Paper No. 2000-4126, 18th Applied Aerodynamics Conference, Denver, Colorado, USA, August 2000.
5. Forrest, J. S. and Owen, I., "An Investigation of Ship Airwakes Using Detached-Eddy Simulation," Computers & Fluids, 2010, 39 (4), 656–673.
6. Carico, G.D., Fang, R., Finch, R.S., Geyer Jr, W.P., Krijins, H.W. and Long, K. "Helicopter/Ship Qualification Testing". NATO SCI-055 Task Group, RTO-AG-300 Vol 22, February 2003.
7. Roscoe, M. and Wilkinson, C.H., "DIMSS – JSHIP's modelling and simulation process for ship/helicopter testing & training", Proc. AIAA Modelling & Simulation Technologies Conference, Monterey, CA, AIAA 2002-4597.
8. Forrest, S.J., Owen, I., Padfield, G.D. and Hodge, S.J., "Ship-helicopter operating limits prediction using piloted flight simulation and time-accurate airwakes", J. Aircraft, 2012, 49 (4), 1020-1031.
9. Hodge, S.J., Forrest, J.S., Padfield, G.D. and Owen I., "Simulating the Environment at the Helicopter-Ship Dynamic Interface: Research, development and Application", Aeronautical J., 2012, 116 (1185), 2012, 1155-1184.
10. White, M.D., Perfect, P., Padfield, G.D., Gubbels, A.W. and Berryman, A.C., "Acceptance testing and commissioning of a flight simulator for rotorcraft simulation fidelity research", Proc. IMechE Part G: J Aerospace Engineering, 2012, 226(4), 638-686.
11. Scott, P., White, M.D. and Owen, I., "The effect of ship size on airwake aerodynamics and maritime helicopter operations", 41st European Rotorcraft Forum, Munich, 1-4 September 2014.
12. McRuer, D.T. "Interdisciplinary interactions and dynamic systems integration", Int J Control, 1994, Vol. 59, 3-12.
13. Scott, P., Owen, I. and White, M.D., "The Effect of ship size on the flying qualities of maritime helicopters", American Helicopter Society 70th Annual Forum, Montreal, Canada, May 20-22, 2014.
14. McTaggart, K., "Validation of ShipMo3D Version 1.0 User Applications for Simulation of Ship Motion", Technical Memorandum, DRDC Atlantic TM 2007-173, August 2007.
15. McTaggart, K.A. and Langlois, R.G., "Physics-Based Modelling of Ship Replenishment at Sea Using Distributed Simulation", Society of Naval Architects and Marine Engineers Annual Meeting and Expo, Providence, Rhode Island, USA, 20-23 October 2009.
16. ITTC Seakeeping Committee Report. In 15th International Towing Tank Conference, Vol. 1, pp. 55–114. The Hague, 1978.
17. Cummins, W.E. and Bales, S.L., "Extreme value and rare occurrence statistics for Northern Hemisphere shipping lanes", 1980 SNAME Spring Meeting and STAR Symposium, California, USA, 3-7 June 1980.
18. Duval, R.W. "A real-time multi-body dynamics architecture for rotorcraft simulation," in RAeS Proceedings of the challenge of realistic rotorcraft simulation, London, UK, 7-8 November, 2001.
19. Roscoe, A. H., and Ellis, G. A., "A Subjective Ratings Scale for Assessing Pilot Workload in Flight: A Decade of Practical Use," RAE, TR TR90019, 1990.
20. Finlay, B.A. "Ship Helicopter Operating Limit Testing – Past, Present and Future", RAeS Rotorcraft Group Conference on 'Helicopter Operations in the Maritime Environment', London, UK, March 2001.